Article

Fluorescence Spectroscopy and Chemometrics: A Simple and Easy Way for the Monitoring of Fluoroquinolone Mixture Degradation

Iván Sciscenko, Hoàng Thị Mỹ Hắng, Carlos Escudero-Oñate, Isabel Oller, and Antonio Arques*

Read Online

ACCESS | Metrics & More | Article Recommendations | Supporting Information

ABSTRACT: In this work, fluorescence excitation−emission matrices (EEMs), in combination with the chemometric tool and parallel factor analysis (PARAFAC), have been proposed as an unexplored methodology to follow the removal of the fluorescent contaminants of emerging concern, fluoroquinolones (FQs). Ofloxacin, enrofloxacin, and sarafloxacin were degraded by different advanced oxidation processes employing simulated sunlight ($h\nu$): photolysis, $H_2O_2/h\nu$, and photo-Fenton. All experiments were performed in ultrapure water at three different pH values: 2.8, 5.0, and 7.0. With the obvious advantage of multivariate analysis methods, EEM-PARAFAC allowed the monitoring of degradation from the overall substances (original and formed ones) through simultaneous, rapid, and cost-efficient fluorescence spectroscopy determinations. A five-component model was found to best fit the experimental data, allowing us to (i) describe the decay of the fluorescence signals of the three parent pollutants, (ii) follow the kinetics profile of FQ-like byproducts with similar EEM fingerprints than the original FQs, and (iii) observe the formation of two families of reaction intermediates with completely different EEMs. Results were finally correlated with high pressure liquid chromatography, total organic carbon, and toxicity tests on *Escherichia coli*, showing good agreement with all the studied techniques.
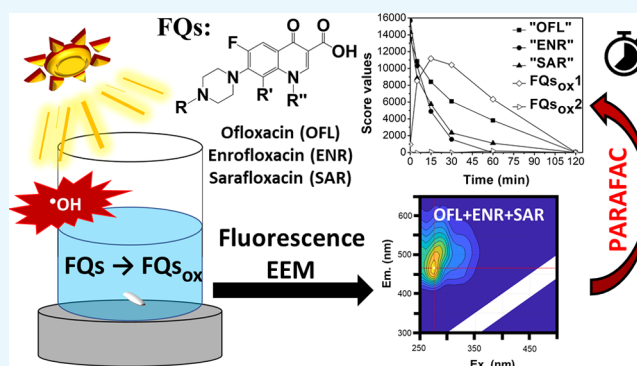
1. INTRODUCTION

Advanced oxidation processes (AOPs) have been demonstrated to be useful to degrade pharmaceuticals and other so-called contaminants of emerging concern (CECs).[1−3] Within this field, analytical techniques such as high pressure liquid chromatography (HPLC) and high-resolution mass spectrometry were mainly employed, allowing the user to gain good insights into the CEC removal as well as their oxidation byproduct formation.[4,5] However, this kind of technique is sophisticated and expensive. Therefore, research on simpler and cheaper methodologies for AOPs is still meaningful.

Fluoroquinolones (FQs) are one of the most consumed antibiotics in the world.[6] Like most of the antibiotics, they are poorly metabolized by living organisms, thus being commonly found in urban discharges and wastewater treatment plants (WWTPs),[7−10] where they are not efficiently degraded, and thus they constitute a pathway for the incorporation of these substances into ecosystems.[11−14] In addition, FQs could produce proliferation of new bacteria with resistance against these substances[15,16] and toxicity against other aquatic organisms.[17−19] As an extreme example of the presence of these CECs, the case of India must be highlighted, where concentrations in the range of $\mu g/L$, and even mg/L, have been found in WWTPs because of their uncontrolled use and unloading.[20−22]

On the other hand, FQs are fluorescent molecules, thus being advantageous for their determination at low concentrations in complex samples.[23] However, without a separation method such as HPLC, when measuring a single emission fluorescence scan from a solution containing a mixture of these compounds, signals will likely overlap. In order to solve this problem, chemometric tools are required. In this sense, the parallel factor analysis (PARAFAC) is one of the most employed methods within this area, which is capable of decomposing the underlying signals from a fluorescence excitation−emission matrix (EEM) data set.[24] Nevertheless, in addition to other chemometric applications, such as principal component analysis or artificial neural networks, PARAFAC requires a solid programming background, which might be its major drawback. Till date, however, because EEM-PARAFAC usage is rapidly rising, free graphical user interfaces have been developed.[25,26]

So far, EEM-PARAFAC has been mainly employed in the characterization of complex water samples containing naturally
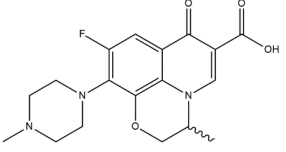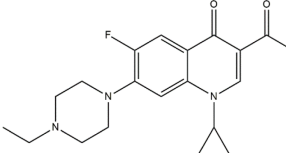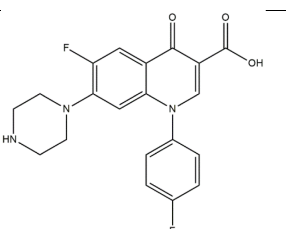
Table 1. Molecular Structure and pK_a Values of the studied FQs[a]

Fluoroquinolone	Structure	pKa$_1$	pKa$_2$
Ofloxacin (OFL)		5.98	8.00
Enrofloxacin (ENR)		6.20	8.13
Sarafloxacin (SAR)		5.91	9.07

[a]According to values reported by Van Doorslaer et al.[9]

dissolved organic matter,[27,28] as well as for monitoring the organic matter in a WWTP,[29,30] and more recently, it has been also applied in CEC degradation studies.[31,32] In addition to this, it has also been previously employed in combination with routine HPLC analysis and different bioassays to get a better understanding of the transformation of a FQ, enrofloxacin (ENR), under different (photo)-oxidative conditions.[33] However, application of this methodology to more complex samples remains, as far as we know, unexplored. Analyzing the changes within the fluorescence matrices, not only qualitatively, but measuring the different components (identified as original pollutants and reaction intermediates) in a mixture of three FQs is challenging, as it would confirm EEM-PARAFAC as a powerful tool to gain insights into the behavior of the sample, avoiding the use of expensive and sophisticated tools, which are not always available.

With this background, in this work, the degradation of three FQs with a high occurrence in water bodies is reported. Ofloxacin (OFL), ENR, and sarafloxacin (SAR) will be simultaneously determined by a time-course EEM with the subsequent PARAFAC analysis. Treatment of the mixture by solar-simulated photo-Fenton has been studied and compared with the corresponding controls: photolysis, $H_2O_2/h\nu$, and Fenton (Fe/H_2O_2).[34] The process will be also followed by the most commonly employed techniques: HPLC for pollutant removal, mineralization by total organic carbon (TOC), and antibacterial activity decay by the zone of inhibition halo test with *Escherichia coli*. Finally, the possible correlations between the different information extracted from all the applied methodologies will also be investigated.

2. EXPERIMENTAL SECTION

2.1. Reagents. OFL, ENR, and SAR (Table 1) of high purity (>99%) and catalase (lyophilized powder from bovine liver 2000−5000 units/mg protein) were purchased from Sigma-Aldrich. Na$_2$SO$_3$ anhydride (85−90%), FeSO$_4$·7H$_2$O, H$_2$O$_2$ (33% w/v), ascorbic acid, 1,10-phenanthroline 1-hydrate,

H$_2$SO$_4$ (96% w/w), and UHPLC-grade methanol and acetonitrile were obtained from AppliChem-Panreac. Formic acid (80% w/w) was purchased from VWR Chemicals. Ultrapure water was prepared with a Merck Milli-Q system. The zone of inhibition tests was made using *E. coli* CECT 101 strain, employing tryptone soya and Mueller−Hinton broth, both provided by Scharlau.

2.2. Solar Simulator Photoreactor. Experiments were carried out in an open batch reactor (total volume 500 mL), loaded with 250 mL of the FQ mixture, consisting of 8 mg/L of each of the compounds, OFL, ENR, and SAR. This concentration is above the values commonly found in ecosystems, but it allows for better monitoring of the process (e.g., accurate kinetic data, reliable values of mineralization). Besides, AOPs can also be used for the concentrate stream treatment after membrane processes, where high concentrations of CEC are expected.[35]

Irradiations were performed with a solar simulator Oriel Instrument, equipped with a high-pressure Xe lamp (Ushio UXL-302-0). The initial pH values of the solutions were adjusted to 2.8, 5.0, and 7.0 by dropwise addition of H$_2$SO$_4$ 0.5 M and/or NaOH 1 M. When required, 125 mg/L of H$_2$O$_2$ was added, which accounts for the total stoichiometric amount needed to mineralize the three FQs, to prevent exhaustion of this reagent during the reaction. For the (photo)-Fenton experiments, 5 mg/L Fe(II), as FeSO$_4$·7H$_2$O salt, was added to the reactor. All the assays were carried out for 120 min, taking samples in time intervals and processed differently depending on the type of analysis, as described in the "Sample Preparation" section.

FQ mixture solution has proved to be stable in the dark under each of the studied pH values, and the addition of H$_2$O$_2$ did not produce further degradation. Comprehensively, the Fe(II)/H$_2$O$_2$ system in dark conditions (Fenton reaction) produced considerable FQ degradation, as described in the "Results and Discussion" section.

2.3. Sample Preparation.

For HPLC and EEM measurements, all samples contained H_2SO_4 5.0 mM (to provide acidic media for all the analysis) and methanol 0.25 M to quench the excess H_2O_2 and ensure that the Fenton reaction has stopped.[36] For TOC determinations, excess Na_2SO_3 was used to get rid of hydrogen peroxide in order to avoid interferences caused by the addition of extra organic substances. In antibacterial activity assays, all samples were first adjusted to pH 7.0 with 1 M NaOH, and afterward, excess catalase enzyme was added to eliminate the remaining H_2O_2.

2.4. Chemical and Toxicological Determinations.

The removal of OFL, ENR, and SAR was determined by HPLC analysis using a Hitachi Chromaster apparatus with a UV/vis detector. A C18 Machery-Nagel column Nucleodur-π^2 5 μm was used as the stationary phase, and an isocratic flow of 0.25 mL/min of formic acid 0.1 M 80% and acetonitrile 20% was used as the eluent. The column oven was set at 40 °C, and the detection was performed at 285 nm. Mineralization measurements were performed in a Shimadzu TOC-V equipment with an ASI-V autosampler. Fluorescence was measured in a Horiba PTI Quanta Master 400 spectrofluorometer, equipped with a Xe arc lamp. EEMs were recorded within the excitation range of 250−500 and the emission range of 300−650 nm (both recorded within 5 nm intervals). Inner filter effect corrections (250−650 nm) were performed with a Hitachi-UH5300 spectrophotometer. The same device was used to measure the dissolved Fe(II) and total iron content, according to the ISO 6332:1988 standardized method with the 1,10-phenanthroline reagent. Antibacterial activity assays were performed employing *E. coli* bacteria, which was previously grown in a nutrient media for 18 h. The colonies were inoculated in a tryptone soya broth, having a suspension of 0.5 units in the McFarland scale. A sterile cotton swab was used to pick bacterial suspension and spread it on the surface of the Mueller−Hinton agar in the petri dish. Then, 0.85 cm wells were made and filled with 100 μL of the sample. Finally, the petri dishes were incubated at 37 °C for 24 h before measuring the zone of inhibition diameters.

2.5. PARAFAC Analysis.

PARAFAC analysis was performed employing Matlab2018b with the free graphical user interface EEMlab.[25] When needed, samples were previously diluted accordingly, with the initial samples being diluted at a 1:20 ratio and diminishing this factor proportionally with degradation time. The analyzed data set consisted of 118 absorbance spectra and EEM (also including the ones belonging to the individual FQs, as shown in Figure 3A) and 14 blanks. The intensity standardization was carried out using the water Raman scatter peak at 350 nm excitation wavelength, thus also being added to the data set 14 water Raman scans.[37]

During the preprocessing stage, EEMs with negligible fluorescence signals were treated as outliers, and thus they were eliminated. The first-order Rayleigh scatter band was corrected with missing values, and second-order Rayleigh and both Raman scatter bands were handled by interpolation. EEMs were always normalized prior to any PARAFAC analysis, so that all samples contained similar weighting. Once the best model was chosen, normalization was reversed.

The number of components (underlying fluorophores) was assessed according to the chemical consistency of the obtained data, residual distribution, and the core consistency diagnostic (CORCONDIA)[38] (see Figure S1 and Table S1).

3. RESULTS AND DISCUSSION

3.1. Photolysis with and without H_2O_2 Addition.

The first series of experiments were devoted to check the stability of FQs versus photolysis with simulated sunlight at different pH values, 2.8, 5.0, and 7.0 (Figure 1A−C, respectively). Noticeable
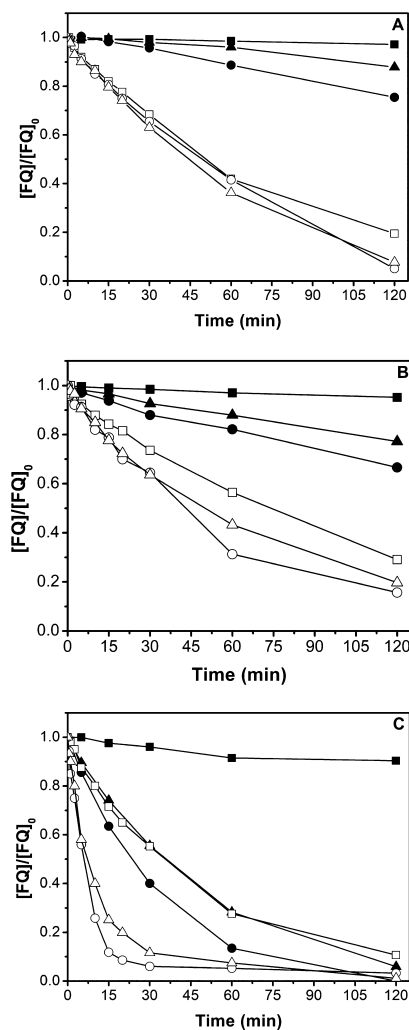
Figure 1. Degradation kinetics of the three studied FQs (8 mg/L each) under simulated sunlight irradiation ($h\nu$) and also with the addition of H_2O_2 125 mg/L ($H_2O_2/h\nu$) at initial pH: (A) 2.8, (B) 5.0, and (C) 7.0. $h\nu$: OFL (■), ENR (●), and SAR (▲); $H_2O_2/h\nu$: OFL (□), ENR (○), and SAR (△).

antibiotic removal was observed, following the trend ENR > SAR > OFL, in agreement with other works;[39,40] this might be indicated by the presence of electron-donating groups in the meta position with respect to the fluoride, where in this case, only OFL has it (Table 1).[41] Besides, the highest removals were obtained at pH 7.0, evidencing the fact that FQ photolysis rates are not only structure-dependent, but pH-dependent as well. Because at pH = 7.0 the neutral/zwitterionic ionization form of the FQs are predominating according to pK_a given in Table 1, these species suffer from faster photolysis than the cationic form that can be found at pH 2.8 or 5.0, which is in line with the other works reporting higher photolytic quantum yields for FQ neutral forms than the cationic ones.[42,43]

When H_2O_2 125 mg/L was added into the system with sunlight irradiation, it enhanced FQ degradation in all cases. At

pH 2.8 (Figure 1A), OFL, ENR, and SAR reached the 50% degradation in ca. 45 min, whereas in the analogous case, without the H_2O_2 addition, the removal percentage obtained at that time was lower than 10%. Therefore, two issues are relevant: (1) faster removals are related to the effect of higher $^{\bullet}OH$ concentration produced *in situ* by H_2O_2 dissociation from photon absorption within the UV region of the Xe emission spectra[44] and (2)because bimolecular kinetic constants rates between $^{\bullet}OH$ and OFL are comparable to the other FQs (at pH 7.0, $9 \pm 2 \times 10^9\ M^{-1}\ s^{-1}$ for OFL, $10 \pm 3 \times 10^9\ M^{-1}\ s^{-1}$ for ENR, and $12 \pm 3 \times 10^9\ M^{-1}\ s^{-1}$ for SAR),[40] there are no significant differences between OFL and ENR or SAR, contrary to what was observed with light irradiation alone. A comparable trend was obtained at pH 5.0 (Figure 1B).

On the other hand, at pH 7.0, OFL showed again higher stability than ENR and SAR (Figure 1C), most probably because of the high contribution of the photolysis process at this pH, where, as stated above, OFL showed a more refractory behavior than the other two FQs.

3.2. Fenton and Photo-Fenton Treatments. Dark Fenton at pH 2.8 was able to remove the FQs in only 20 min (Figure 2A). As expected, a decrease in the reaction efficiency was observed with an increasing pH value: at pH = 5.0 ca. Two hours was required for the elimination of the FQs, while at pH = 7.0, the removal was scarce (Figure 2B,C). In general, changes in the reactivity of the different pollutants were negligible, attributable to the similar kinetic rate constants of $^{\bullet}OH$ with the three FQs mentioned in the previous section.

The irradiation with simulated sunlight resulted in an enhancement of the process (photo-Fenton). At pH = 2.8, the FQs were eliminated in only 5 min. Interestingly, the reaction was still very fast at pH = 5.0, as observed previously for the ENR alone.[33] This is a very important result in view of the real implementation of the process, as strong acidification of the solution can be overcome without the need for adding extra chemicals, such as iron-chelating agents.[27,45] This result is attributable to the ability of FQs to form stable complexes [formation constant rate between 45 and 50 with stoichiometry 3:1 FQ/Fe(III),[46] which are able to extend a photo-Fenton-like process to higher pH domains,[33] even until neutral pH (see Table S2). In sharp contrast to pH 5.0, as it can be observed by comparing Figures 1C and 2C, at pH = 7.0, Fe(II)/H_2O_2/$h\nu$ was less efficient than H_2O_2/$h\nu$. This means that, first, even though there is significant iron in aqueous solution, photo-Fenton seems to be no longer efficient at this pH, and on the other hand, that FQ−iron complex might be more stable against photolysis than the antibiotic itself, as it has been reported for other FQ/metal complexes.[47,48] Because of these statements, the photodegradation contribution to their overall removal is, therefore, lower, thus explaining the faster removals obtained in the case without iron.

3.3. EEM-PARAFAC Analysis. *3.3.1. PARAFAC Model.* Although FQs were degraded by most of the studied processes and experimental conditions, only with photo-Fenton at acidic pH, significant mineralization was evidenced. Under these conditions, after 2 h, 77 and 62% TOC decrease was achieved at pH 2.8 and 5.0, respectively, being negligible in all the other cases (Figure S2). These results are indicative of a large formation of transformation products along with the oxidative reaction. In order to analyze the FQ degradation and their byproduct formation in an innovative and cheaper way, EEMs were measured and then processed with PARAFAC, decomposing each fluorescence matrix into its individual components.
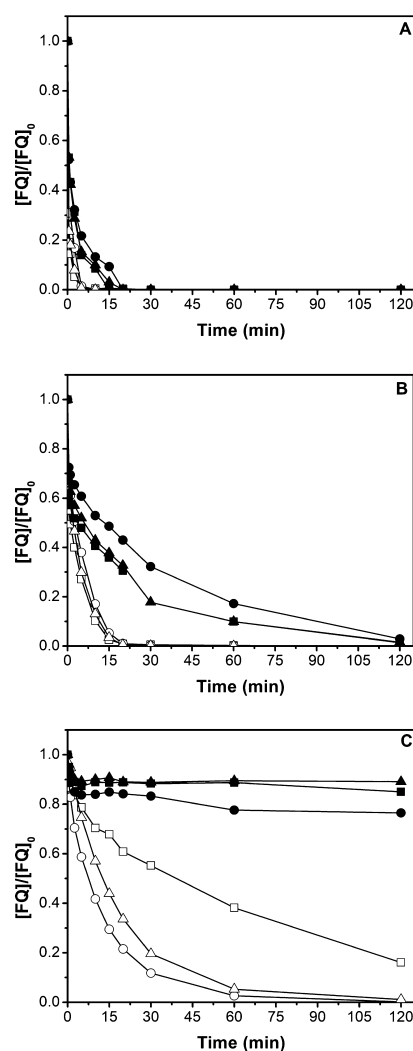

Figure 2. (Photo)-Fenton degradation kinetics for the three studied FQs (8 mg/L each) at initial pH: (A) 2.8, (B) 5.0, and (C) 7.0. Fenton: OFL (■), SAR (▲), and ENR (●); photo-Fenton: OFL (□), ENR (○), and SAR (Δ).

This procedure has been already tested to investigate the degradation of ENR alone, but the system here investigated is more complex because it involves a mixture of three parent compounds with very similar molecular structures.

A set of 118 EEMs were considered in this study, obtained from the sampling at different times during the tested AOPs. As described in the Experimental Section, a model consisting of 5 components was chosen. Figure 3A shows the EEM from the individual FQs together with their mixture, and in Figure 3B, the modeled fingerprints obtained from the PARAFAC model are shown.

The first three components of the model (C1-3) can be associated with the parent pollutants, OFL, ENR, and SAR, respectively, although the contribution of some byproducts with a similar structure cannot be disregarded. Component C4 exhibited shifts toward shorter excitation wavelengths (<250 nm), but remained close to the FQ's emission range, ca. 480 nm. On the other hand, C5 showed a big emission shift close to 390 nm, which can be associated to deeper changes in the molecule than C4, such as cleavage of their piperazine side chain, as it is the group which mainly modulates the FQ fluorescence spectra.[41,49]
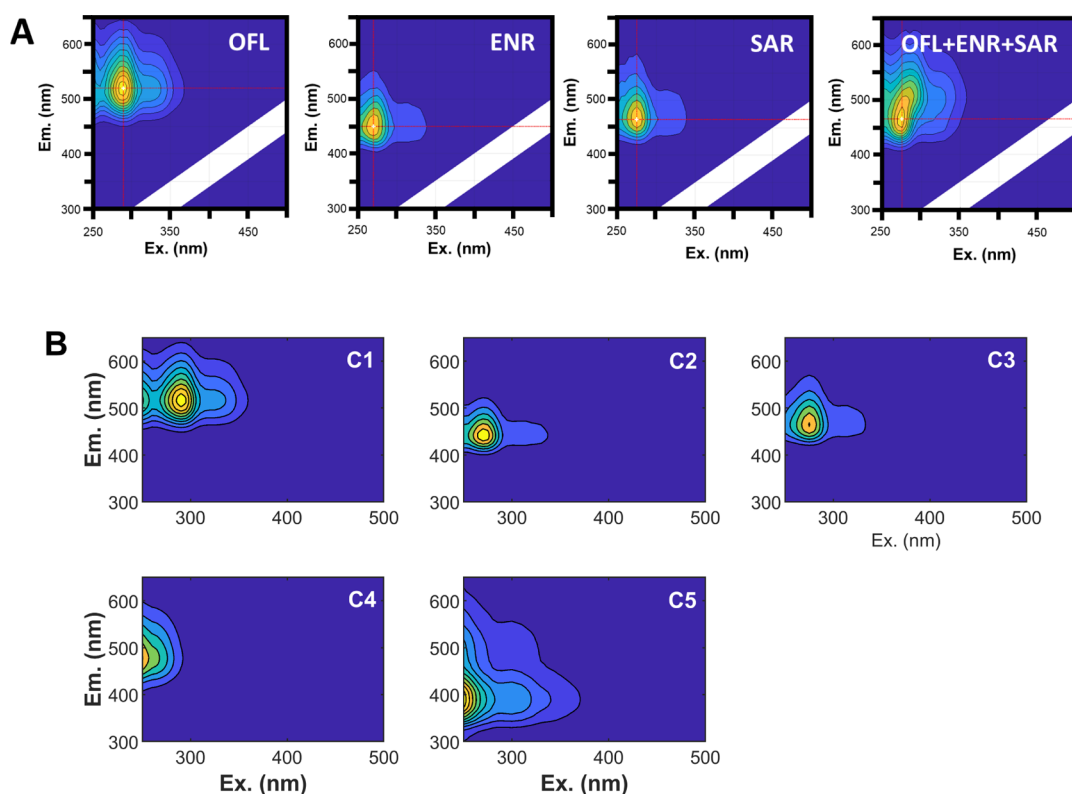
Figure 3. (A) Normalized EEMs after their preprocessing with EEMlab and (B) five-component fingerprints from the EEM-PARAFAC analysis.
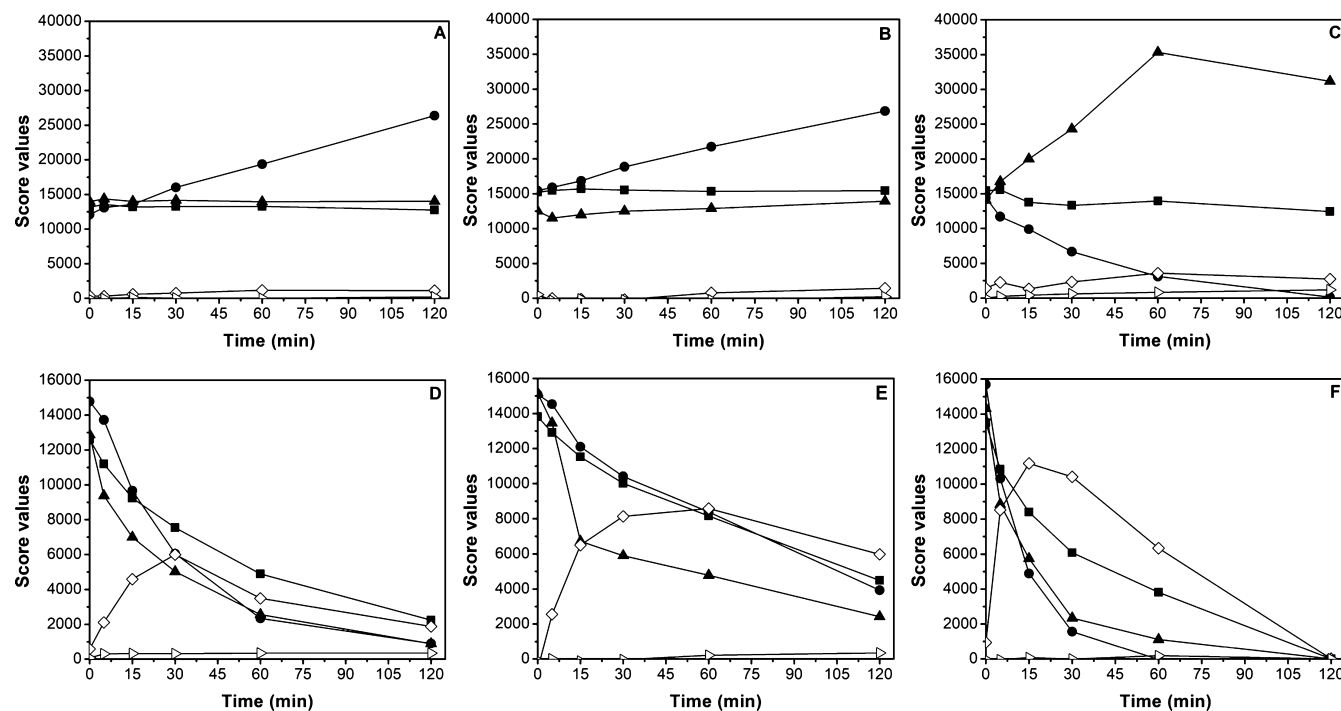
Figure 4. OFL, ENR, and SAR (8 mg/L each) degradation with light irradiation followed by EEM-PARAFAC (5-component model) methodology at pH (A) 2.8, (B) 5.0, and (C) 7.0, and with H_2O_2 125 mg/L addition at pH (D) 2.8, (E) 5.0, and (F) 7.0. PARAFAC component representation: C1 (■), C2 (●), C3 (▲), C4 (◇), and C5 (▷).

3.3.2. PARAFAC Components Evolution after hν and H₂O₂/ hν. Based on EEM-PARAFAC analysis, the variation of each component was followed. At pH 2.8 and 5.0, a negligible decrease in C1 and C3 score values was observed. However, some increase in C2 was recorded, most probably associated with components with similar EEM as ENR but with a higher fluorescence quantum yield that cannot be resolved by the model (Figure 4A,B). On the contrary, at pH = 7.0, decrease in C1 and C2 was monitored with an increase in C3 (Figure 4C). In this case, the destruction of C1 and C2 structures and
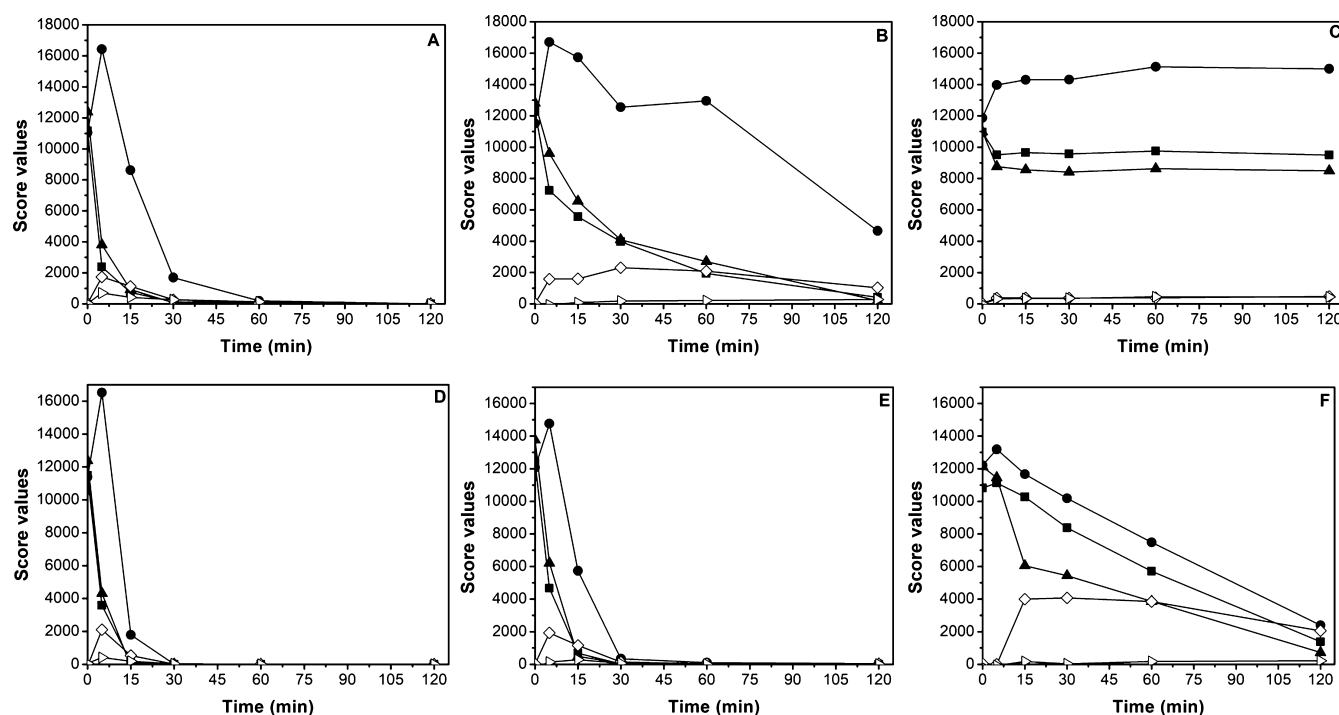
Figure 5. OFL, ENR, and SAR (8 mg/L each) degradation followed by EEM-PARAFAC (5-component model) methodology with the Fenton process at pH (A) 2.8, (B) 5.0, and (C) 7.0 and photo-Fenton at pH (D) 2.8, (E) 5.0, and (F) 7.0. In all cases, $[H_2O_2]_0$ = 125 mg/L and $[Fe(II)]_0$ = 5 mg/L. PARAFAC components representation: C1 (■), C2 (●), C3 (▲), C4 (◇), and C5 (▷).

concomitant release of new photoproducts have to be hypothesized; a tentative explanation could be that the photoproducts formed from OFL, ENR, and SAR degradations should emit within the region of C3. C4 and C5 score values were negligible in all cases, indicating that photolysis resulted in scarce modification of the FQ molecule. These observations show that in agreement with HPLC results, not only FQ photolytic kinetics are pH-dependent but also their photo-degradation pathways.

When H_2O_2 was added under irradiation, the sample fluorescence exhibited a faster decay (Figure 4D−F). Also, in this case, significant differences were observed between pH 7.0 and acidic conditions. Analyzing the components related to the parent pollutants, at pH 2.8 and 5.0, C1 and C2 presented decay of similar score values, whereas the faster ones were obtained for C3, those fitting with SAR's EEM. On the contrary, at pH 7.0, removals followed the same trend than the one obtained with HPLC measurements shown in Figure 1C (ENR > SAR > OFL); thus, C2 > C3 > C1. C4 formation was higher than the one without H_2O_2 addition, which proves a stronger attack to the FQ structure due to the higher photogenerated ●OH, the growth of its score values being faster at neutral pH, in line with the faster decrease of C1−C3.

3.3.3. PARAFAC Component Evolution after Fenton and Photo-Fenton Treatments. Analyzing PARAFAC score value behavior after Fenton and photo-Fenton (Figure 5), C1-3 presented slower removal kinetics than the ones observed for OFL, ENR, and SAR with HPLC-UV/vis (Figure 2). For instance, at pH 2.8, C1-3 disappeared after ca. 15 min, whereas the parent pollutants were degraded in only 5 min. This confirms that products with similar fingerprints as OFL, ENR, and SAR are included in C1−C3 components, as they cannot be completely resolved by the model. As expected, PARAFAC components exhibited a faster decay at pH 2.8, followed by 5.0,

and 7.0, respectively, for Fenton and photo-Fenton. In line with the mineralization results (Figure S2), only for Fenton at pH 2.8, and photo-Fenton at pH 2.8 and 5.0, the fluorescence was negligible at ca. 60 min, in sharp contrast with all other processes where this goal had not been reached.

Regarding the time-course profile of the PARAFAC component, a continuous decrease was observed for both C1 and C3, while a sharp increase was obtained for C2 in the first stages of the process followed by a fast decrease. Once more, this is ought to the formation of products that cannot be solved by the model and that show similar fingerprints to ENR. C4 appeared at the beginning of the process and then disappeared. Similar to the system without iron, C5 formation was always negligible, and in fact, was only visible in the model because of the normalization of the EEM during the preprocessing of the data set (see Experimental Section).

Finally, when comparing Figures 4 and 5, it can be observed that in the last, the initial score values are slightly lower. This is attributed to the chelation with Fe(III) formed through oxidation of Fe(II) in water, diminishing the fluorescence intensity of these compounds (see the example for ENR in Figure S3B and Stern−Volmer plots for each FQ in Figure S4). Although it is an unexpected behavior because coordination complexes generally exhibit greater fluorescence quantum yield than the ligand alone, these observations are in line with the other works reporting FQ fluorescence quenching in presence of Fe(III) and some other transition metals or even with 4-quinolone molecules.[50−52]

Therefore, in order to prove if the Fe presence was an interference for EEM-PARAFAC results, the metal was eliminated prior to the fluorescence measurements and included in the PARAFAC data set. This issue was solved by preparing each sample similarly as described in Section 2.3, but having NaOH 10 mM instead of H_2SO_4 to precipitate iron. Afterward,

samples were flown through PTFE filters 0.45 μm and acidified again in order to measure them in the same condition as all the predecessors.

In Figure S5A,B, PARAFAC score value results for dark Fenton pH 7.0 with iron elimination are shown. Although initial score values did not increase, differences can be observed. For C2, an increment in score values was observed, indicating that iron presence produced quenching of byproducts emitting in this region, and for C3, a slightly faster decay was obtained. For C1, C4, and C5, negligible changes were observed. Nevertheless, the overall trends of the PARAFAC component scores did not change.

3.4. Antibacterial Activity. Antibacterial activity assays were performed for (photo)-Fenton processes and photolysis at pH 2.8, measuring the decay on the diameter of the inhibition halos formed by *E. coli* strains. The results indicated that only for Fenton and photo-Fenton processes, *E. coli* started growing again around the wells containing the samples of degradation experiments, thus indicating a decrease of the zone of inhibition, whereas it remained constant during the 2 h of the photolysis process.

In Figure 6, the zone of inhibition diameter and the summation of the PARAFAC model components decay, both
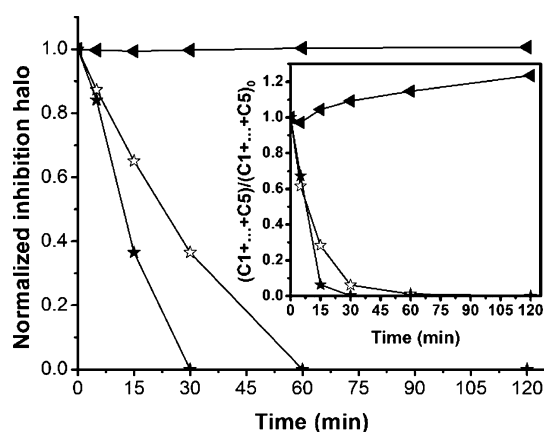
Figure 6. Antibacterial activity decay by *E. coli*-normalized inhibition halo determinations; the insert shows the plot of the summation of component score value (C1 + ... + C5) decay, also normalized, of the FQ mixture (8 mg/L each) at pH 2.8 treated with light irradiation (◄), Fenton (☆), and photo-Fenton (★); in the last two, $[H_2O_2]_0 = 125$ mg/L and $[Fe(II)]_0 = 5$ mg/L.

normalized, is shown. Interestingly, antibacterial activity decay presented the same trend than the disappearance of the 5 PARAFAC components. These results are in line with the ones reported in the previous work,[33] which show that antibacterial ability might be associated with the FQ core.[17,53,54]

4. CONCLUSIONS

The applicability of EEM-PARAFAC as a complementary tool to monitor the behavior of antibiotics in an AOP has been extended to more complex samples, containing mixtures of several parent compounds. Although it was not able to give detailed data on the chemical substances present, it provides valuable information on the behavior of the FQ core that can be related with toxicity.

According to the abovementioned results, three interesting tasks should be addressed in the next future for a better understanding of the process: (a) investigate the nature of the interaction between Fe and the FQs to explain the good performance of photo-Fenton at mild pH, (b) to combine EEM-PARAFAC with smart HPLC-mass spectrometry analysis to correlate the components obtained in the mathematical model with a compound or group of compounds, and (c) to explore the real applicability of the methodology here developed with lower pollutant concentrations (e.g., μg/L), using different aqueous matrices (role of salinity and dissolved organic matter) and scaling it up to higher volumes using real sunlight as the irradiation source.

◼ ASSOCIATED CONTENT

Ⓢ Supporting Information

The Supporting Information is available free of charge at https://pubs.acs.org/doi/10.1021/acsomega.0c05370.

> EEM-PARAFAC residuals and CORCONDIA results; total organic carbon measurements; total iron concentration measurements in the photo-Fenton process at the three studied pH values; and ENR fluorescence quenching by Fe(III) (PDF)

◼ AUTHOR INFORMATION

Corresponding Author

> **Antonio Arques** — *Departamento de Ingeniería Textil y Papelera, Universitat Politècnica de València (UPV), 46022 Valencia, Spain;* ⓘ orcid.org/0000-0001-8692-6979; Email: aarques@txp.upv.es

Authors

> **Iván Sciscenko** — *Departamento de Ingeniería Textil y Papelera, Universitat Politècnica de València (UPV), 46022 Valencia, Spain;* ⓘ orcid.org/0000-0003-1112-8512
> **Hoàng Thị Mỹ Hằng** — *Hue University of Sciences, 530000 Thừa Thiên Huê, Vietnam*
> **Carlos Escudero-Oñate** — *Institute for Energy Technology (IFE), 2007 Kjeller, Norway*
> **Isabel Oller** — *Plataforma Solar de Almería-CIEMAT, 04200 Tabernas, Spain*

Complete contact information is available at:
https://pubs.acs.org/10.1021/acsomega.0c05370

Author Contributions

The manuscript was written through contributions of all authors. All authors have given approval to the final version of the manuscript.

Notes

The authors declare no competing financial interest.

◼ ACKNOWLEDGMENTS

◼ ABBREVIATIONS

AOPs, advanced oxidation processes; CEC, contaminant of emerging concern; CORCONDIA, core consistency diagnostic; ENR, enrofloxacin; EEM, excitation-emission matrix; FQ, fluoroquinolone; HPLC, high pressure liquid chromatography; OFL, ofloxacin; PARAFAC, parallel factor analysis; SAR,

sarafloxacin; TOC, total organic carbon; WWTP, wastewater treatment plant

■ REFERENCES

(1) Buxton, G. V.; Greenstock, C. L.; Helman, W. P.; Ross, A. B. Critical Review of Rate Constants for Reactions of Hydrated Electrons, Hydrogen Atoms and Hydroxyl Radicals (·OH/·O −) in Aqueous Solution. *J. Phys. Chem. Ref. Data* **1988**, *17*, 513−886.

(2) Fujishima, A.; Rao, T. N.; Tryk, D. A. Titanium Dioxide Photocatalysis. *J. Photochem. Photobiol., C* **2000**, *1*, 1−21.

(3) Salimi, M.; Esrafili, A.; Gholami, M.; Jonidi Jafari, A.; Rezaei Kalantary, R.; Farzadkia, M.; Kermani, M.; Sobhi, H. R. Contaminants of Emerging Concern: A Review of New Approach in AOP Technologies. *Environ. Monit. Assess.* **2017**, *189*, 414.

(4) Villegas-Guzman, P.; Oppenheimer-Barrot, S.; Silva-Agredo, J.; Torres-Palma, R. A. Comparative Evaluation of Photo-Chemical AOPs for Ciprofoxacin Degradation: Elimination in Natural Waters and Analysis of PH Effect, Primary Degradation By-Products, and the Relationship with the Antibiotic Activity. *Water, Air, Soil Pollut.* **2017**, *228*, 209−224.

(5) Malato, S.; Fernández-Ibáñez, P.; Maldonado, M. I.; Blanco, J.; Gernjak, W. Decontamination and Disinfection of Water by Solar Photocatalysis: Recent Overview and Trends. *Catal. Today* **2009**, *147*, 1−59.

(6) Hamad, B. The Antibiotics Market. *Nat. Rev. Drug Discovery* **2010**, *9*, 675−676.

(7) Gao, L.; Shi, Y.; Li, W.; Niu, H.; Liu, J.; Cai, Y. Occurrence of Antibiotics in Eight Sewage Treatment Plants in Beijing, China. *Chemosphere* **2012**, *86*, 665−671.

(8) Kümmerer, K. The Presence of Pharmaceuticals in the Environment Due to Human Use - Present Knowledge and Future Challenges. *J. Environ. Manage.* **2009**, *90*, 2354−2366.

(9) Van Doorslaer, X.; Dewulf, J.; Van Langenhove, H.; Demeestere, K. Fluoroquinolone Antibiotics: An Emerging Class of Environmental Micropollutants. *Sci. Total Environ.* **2014**, *500−501*, 250−269.

(10) Sukul, P.; Spiteller, M. Fluoroquinolone Antibiotics in the Environment. *Reviews of Environmental Contamination and Toxicology*, 2007; Vol. *191*, pp 131−62.

(11) Silva, B. F. d.; Jelic, A.; López-Serna, R.; Mozeto, A. A.; Petrovic, M.; Barceló, D. Occurrence and Distribution of Pharmaceuticals in Surface Water, Suspended Solids and Sediments of the Ebro River Basin, Spain. *Chemosphere* **2011**, *85*, 1331−1339.

(12) Hoang, T. T. T.; Tu, L. T. C.; Le, N. P.; Dao, Q. P.; Trinh, P. H. Fate of Fluoroquinolone Antibiotics in Vietnamese Coastal Wetland Ecosystem. *Wetlands Ecol. Manage.* **2012**, *20*, 399−408.

(13) Thuy, H. T. T.; Nga, L. P.; Loan, T. T. C. Antibiotic Contaminants in Coastal Wetlands from Vietnamese Shrimp Farming. *Environ. Sci. Pollut. Res.* **2011**, *18*, 835−841.

(14) He, X.; Wang, Z.; Nie, X.; Yang, Y.; Pan, D.; Leung, A. O. W.; Cheng, Z.; Yang, Y.; Li, K.; Chen, K. Residues of Fluoroquinolones in Marine Aquaculture Environment of the Pearl River Delta, South China. *Environ. Geochem. Health* **2012**, *34*, 323−335.

(15) Petchiappan, A.; Chatterji, D. Antibiotic Resistance: Current Perspectives. *ACS Omega* **2017**, *2*, 7400−7409.

(16) Rutgersson, C.; Fick, J.; Marathe, N.; Kristiansson, E.; Janzon, A.; Angelin, M.; Johansson, A.; Shouche, Y.; Flach, C.-F.; Larsson, D. G. J. Fluoroquinolones and Qnr Genes in Sediment, Water, Soil, and Human Fecal Flora in an Environment Polluted by Manufacturing Discharges. *Environ. Sci. Technol.* **2014**, *48*, 7825−7832.

(17) Aristilde, L.; Melis, A.; Sposito, G. Inhibition of Photosynthesis by a Fluoroquinolone Antibiotic. *Environ. Sci. Technol.* **2010**, *44*, 1444−1450.

(18) Ziarrusta, H.; Mijangos, L.; Irazola, M.; Prieto, A.; Etxebarria, N.; Anakabe, E.; Olivares, M.; Zuloaga, O. Ciprofloxacin By-Products in Seawater Environment in the Presence and Absence of Gilt-Head Bream. *Chemosphere* **2018**, *197*, 560−568.

(19) Robinson, A. A.; Belden, J. B.; Lydy, M. J. Toxicity of Fluoroquinolone Antibiotics to Aquatic Organisms. *Environ. Toxicol. Chem.* **2005**, *24*, 423−430.

(20) Rakshit, S.; Sarkar, D.; Elzinga, E. J.; Punamiya, P.; Datta, R. Mechanisms of Ciprofloxacin Removal by Nano-Sized Magnetite. *J. Hazard. Mater.* **2013**, *246−247*, 221−226.

(21) Larsson, D. G. J.; de Pedro, C.; Paxeus, N. Effluent from Drug Manufactures Contains Extremely High Levels of Pharmaceuticals. *J. Hazard. Mater.* **2007**, *148*, 751−755.

(22) Gothwal, R.; Shashidhar. Occurrence of High Levels of Fluoroquinolones in Aquatic Environment Due to Effluent Discharges from Bulk Drug Manufacturers. *J. Hazard., Toxic Radioact. Waste* **2017**, *21*, 05016003.

(23) Aufartová, J.; Brabcová, I.; Torres-Padrón, M. E.; Solich, P.; Sosa-Ferrera, Z.; Santana-Rodríguez, J. J. Determination of Fluoroquinolones in Fishes Using Microwave-Assisted Extraction Combined with Ultra-High Performance Liquid Chromatography and Fluorescence Detection. *J. Food Compos. Anal.* **2017**, *56*, 140−146.

(24) Murphy, K. R.; Stedmon, C. A.; Graeber, D.; Bro, R. Fluorescence Spectroscopy and Multi-Way Techniques. PARAFAC. *Anal. Methods* **2013**, *5*, 6557−6566.

(25) Micó, P.; García-Ballesteros, S.; Mora, M.; Vicente, R.; Amat, A. M.; Arques, A. A Graphical User-Friendly Interface for Fluorimetry Experiments Based on the DrEEM Toolbox. *Chemom. Intell. Lab. Syst.* **2019**, *188*, 6−13.

(26) Mazivila, S. J.; Bortolato, S. A.; Olivieri, A. C. MVC3_GUI: A MATLAB Graphical User Interface for Third-Order Multivariate Calibration. An Upgrade Including New Multi-Way Models. *Chemom. Intell. Lab. Syst.* **2018**, *173*, 21−29.

(27) García-Ballesteros, S.; Grimalt, J.; Berto, S.; Minella, M.; Laurenti, E.; Vicente, R.; López-Pérez, M. F.; Amat, A. M.; Bianco Prevot, A.; Arques, A. New Route for Valorization of Oil Mill Wastes: Isolation of Humic-Like Substances to Be Employed in Solar-Driven Processes for Pollutants Removal. *ACS Omega* **2018**, *3*, 13073−13080.

(28) Cuss, C. W.; McConnell, S. M.; Guéguen, C. Combining Parallel Factor Analysis and Machine Learning for the Classification of Dissolved Organic Matter According to Source Using Fluorescence Signatures. *Chemosphere* **2016**, *155*, 283−291.

(29) Henderson, R. K.; Baker, A.; Murphy, K. R.; Hambly, A.; Stuetz, R. M.; Khan, S. J. Fluorescence as a Potential Monitoring Tool for Recycled Water Systems: A Review. *Water Res.* **2009**, *43*, 863−881.

(30) Yang, L.; Hur, J.; Zhuang, W. Occurrence and Behaviors of Fluorescence EEM-PARAFAC Components in Drinking Water and Wastewater Treatment Systems and Their Applications: A Review. *Environ. Sci. Pollut. Res.* **2015**, *22*, 6500−6510.

(31) García-Ballesteros, S.; Mora, M.; Vicente, R.; Vercher, R. F.; Sabater, C.; Castillo, M. A.; Amat, A. M.; Arques, A. A New Methodology to Assess the Performance of AOPs in Complex Samples: Application to the Degradation of Phenolic Compounds by O3 and O3/UV-A−Vis. *Chemosphere* **2019**, *222*, 114−123.

(32) Carabajal, M. D.; Arancibia, J. A.; Escandar, G. M. Excitation-Emission Fluorescence-Kinetic Data Obtained by Fenton Degradation. Determination of Heavy-Polycyclic Aromatic Hydrocarbons by Four-Way Parallel Factor Analysis. *Talanta* **2017**, *165*, 52−63.

(33) Sciscenko, I.; Garcia-Ballesteros, S.; Sabater, C.; Castillo, M. A.; Escudero-Oñate, C.; Oller, I.; Arques, A. Monitoring Photolysis and (Solar Photo)-Fenton of Enrofloxacin by a Methodology Involving EEM-PARAFAC and Bioassays: Role of PH and Water Matrix. *Sci. Total Environ.* **2020**, *719*, 137331.

(34) Pignatello, J. J.; Oliveros, E.; MacKay, A. Advanced Oxidation Processes for Organic Contaminant Destruction Based on the Fenton Reaction and Related Chemistry. *Crit. Rev. Environ. Sci. Technol.* **2006**, *36*, 1−84.

(35) Miralles-Cuevas, S.; Oller, I.; Pérez, J. A. S.; Malato, S. Removal of Pharmaceuticals from MWTP Effluent by Nanofiltration and Solar Photo-Fenton Using Two Different Iron Complexes at Neutral PH. *Water Res.* **2014**, *64*, 23−31.

(36) Santos-Juanes, L.; García Einschlag, F. S.; Amat, A. M.; Arques, A. Combining ZVI Reduction with Photo-Fenton Process for the Removal of Persistent Pollutants. *Chem. Eng. J.* **2017**, *310*, 484−490.

(37) Lawaetz, A. J.; Stedmon, C. A. Fluorescence Intensity Calibration Using the Raman Scatter Peak of Water. *Appl. Spectrosc.* **2009**, *63*, 936−940.

(38) Bro, R.; Kiers, H. A. L. A New Efficient Method for Determining the Number of Components in PARAFAC Models. *J. Chemom.* **2003**, *17*, 274−286.

(39) Ge, L.; Chen, J.; Wei, X.; Zhang, S.; Qiao, X.; Cai, X.; Xie, Q. Aquatic Photochemistry of Fluoroquinolone Antibiotics: Kinetics, Pathways, and Multivariate Effects of Main Water Constituents. *Environ. Sci. Technol.* **2010**, *44*, 2400−2405.

(40) Ge, L.; Na, G.; Zhang, S.; Li, K.; Zhang, P.; Ren, H.; Yao, Z. New Insights into the Aquatic Photochemistry of Fluoroquinolone Antibiotics: Direct Photodegradation, Hydroxyl-Radical Oxidation, and Antibacterial Activity Changes. *Sci. Total Environ.* **2015**, *527−528*, 12−17.

(41) Albini, A.; Monti, S. Photophysics and Photochemistry of Fluoroquinolones. *Chem. Soc. Rev.* **2003**, *32*, 238−250.

(42) Zhang, Z.; Xie, X.; Yu, Z.; Cheng, H. Influence of Chemical Speciation on Photochemical Transformation of Three Fluoroquinolones (FQs) in Water: Kinetics, Mechanism, and Toxicity of Photolysis Products. *Water Res.* **2019**, *148*, 19−29.

(43) Wammer, K. H.; Korte, A. R.; Lundeen, R. A.; Sundberg, J. E.; McNeill, K.; Arnold, W. A. Direct Photochemistry of Three Fluoroquinolone Antibacterials: Norfloxacin, Ofloxacin, and Enrofloxacin. *Water Res.* **2013**, *47*, 439−448.

(44) Jung, Y. J.; Kim, W. G.; Yoon, Y.; Kang, J.-W.; Hong, Y. M.; Kim, H. W. Removal of Amoxicillin by UV and UV/H2O2 Processes. *Sci. Total Environ.* **2012**, *420*, 160−167.

(45) Santos-Juanes, L.; Amat, A. A.; Arques, A. Strategies to Drive Photo-Fenton Process at Mild Conditions for the Removal of Xenobiotics from Aqueous Systems. *Curr. Org. Chem.* **2017**, *21*, 1074−1083.

(46) Urbaniak, B.; Kokot, Z. J. Analysis of the Factors That Significantly Influence the Stability of Fluoroquinolone-Metal Complexes. *Anal. Chim. Acta* **2009**, *647*, 54−59.

(47) Wang, S.; Wang, Z.; Hao, C.; Peijnenburg, W. J. G. M. DFT/TDDFT Insights into Effects of Dissociation and Metal Complexation on Photochemical Behavior of Enrofloxacin in Water. *Environ. Sci. Pollut. Res.* **2018**, *25*, 30609−30616.

(48) Wei, X.; Chen, J.; Xie, Q.; Zhang, S.; Li, Y.; Zhang, Y.; Xie, H. Photochemical Behavior of Antibiotics Impacted by Complexation Effects of Concomitant Metals: A Case for Ciprofloxacin and Cu(II). *Environ. Sci.: Processes Impacts* **2015**, *17*, 1220−1227.

(49) Park, H.-R.; Kim, T. H.; Bark, K.-M. Physicochemical Properties of Quinolone Antibiotics in Various Environments. *Eur. J. Med. Chem.* **2002**, *37*, 443−460.

(50) Park, H.-R.; Oh, C. H.; Lee, H. C.; Choi, J. G.; Jung, B. I.; Bark, K. M. Quenching of Ofloxacin and Flumequine Fluorescence by Divalent Transition Metal Cations. *Bull. Korean Chem. Soc.* **2006**, *27*, 2002−2010.

(51) Ross, D. L.; Riley, C. M. Physicochemical Properties of the Fluoroquinolone Antimicrobials. III. Complexation of Lomefloxacin with Various Metal Ions and the Effect of Metal Ion Complexation on Aqueous Solubility. *Int. J. Pharm.* **1992**, *87*, 203−213.

(52) Gümrükçüoğlu, A.; Topaloğlu, Y.; Mermer, A.; Demirbaş, N.; Demirbaş, A.; Ocak, M.; Ocak, Ü. 4-Quinolone-Carboxamide and Carbothioamide Compounds as Fluorescent Sensors. New Fluorimetric Methods for Cu2+ and Fe3+ Determination in Tap Water and Soil. *J. Fluoresc.* **2019**, *29*, 921−931.

(53) Ge, L.; Halsall, C.; Chen, C.-E.; Zhang, P.; Dong, Q.; Yao, Z. Exploring the Aquatic Photodegradation of Two Ionisable Fluoroquinolone Antibiotics − Gatifloxacin and Balofloxacin: Degradation Kinetics, Photobyproducts and Risk to the Aquatic Environment. *Sci. Total Environ.* **2018**, *633*, 1192−1197.

(54) Shen, L. L.; Mitscher, L. A.; Sharma, P. N.; O'Donnell, T. J.; Chu, D. W.; Cooper, C. S.; Rosen, T.; Pernet, A. G. Mechanism of Inhibition of DNA Gyrase by Quinolone Antibacterials: A Cooperative Drug-DNA Binding Model. *Biochemistry* **1989**, *28*, 3886−3894.